***Original Research Article***

# Submicrostructures of Nephrite from Five Sources Based on Multispectral Imaging and Effect Enhancement

**Abstract:** Some collectors and connoisseurs have found that the nephrite from different sources possess different submicrostructures inside the body, which could become a quite convenient and effective basis for determining provenance. The submicrostructure of nephrite can be observed by the naked eye under irradiated by strong light. However, the images of original submicrostructure of nephrite were recorded by use of multispectral imaging in our previous work, but the visual effect is not satisfied. Here, the main features of different submicrostructures will present more distinct by appropriately subtracting the shining strength and then the average filtering is adopted to promote the resolution of submicrostructure imaging as well as to reduce some image noises. The submicrostructure images of nephrite from five most common sources have typical inherent characteristics respectively, which are qualified to set up a demonstration for identifying provenances. Furthermore, the shape, size, distribution and name for these different submicrostructures have been summarized, and they will become the basis for future research on the provenance of nephrite including the ancient jade..

**Keywords:** Nephrite; Sources; Multispectral image; Average Filter; Submicrostructure



## 1. Introduction

Jade is a type of gem with significant Chinese characteristics and also an important component of Chinese traditional culture. Nephrite is the dominant material of ancient Chinese jade, which is a kind of Ca-silicate mineral with Fe-Mg bearing and double-chain structure. It belongs to an amphbole series between tremolite [$Ca_2Mg_5Si_8O_{22}(OH)_2$] and actinolite [$Ca_2(Mg, Fe^{2+})_5Si_8O_{22}(OH)_2$] (Hawthorne & Oberti, 2006). Thus its color varies from onion-green to greenish-gray, white, pinky, yellowish, tobacco-brown, and bluish to black depending on their iron content and some admixtures of other minerals (serpentine, chlorite, calcite, magnesite, talc, etc.) (Bukanov, 2006). Nephrite petrogenesis has been interpreted to be either metamorphic or metasomatic (Harlow & Sorensen, 2005). The typical nephrite deposit is commonly found at the contacts of gabbros, granitic intrusive rocks, or metamorphic rocks with ultrabasic rocks (Liu *et al.*, 2011).

Jade with oily luster looks fine and smooth. Good hardness and toughness make jade suitable for cutting, polishing and engraving. Compared to jadeite, nephrite has been used and loved for more than 8,000 years of history in China (Yang & Liu, 2017; Wen & Jing, 1992). The nephrite articles are often made into lifelike figures, animal shapes or crystal clear bracelets and pendant ornaments, which can reflect the technological level of different periods and contain rich historical information[6]. However, one of the most basic issues, the provenance of ancient nephrite objects, has always been a controversial topic in the archaeometry field.

Jade ware is handicrafted by pure mechanical operations without any chemical process, thus

**Comment [M1]:**

**Comment [M2]:** sub-microstructures

**Comment [M3]:** sub-microstructures

**Comment [M4]:** sub-microstructure

**Comment [M5]:** sub-microstructures

**Comment [M6]:** sub-microstructure

**Comment [M7]:** sub-microstructure

**Comment [M8]:** sub-microstructures

**Comment [M9]:** sub-microstructures

**Comment [M10]:** amphibole

**Comment [M11]:** “and”

**Comment [M12]:** (Add) and

**Comment [M13]:** magnetite

**Comment [M14]:** meta-somatic

**Comment [M15]:** and

**Comment [M16]:** and”

**Comment [M17]:** and

**Comment [M18]:** Use Standard reference as per other types used

**Comment [M19]:** handcrafted

their trace element compositions should be the same as that of the original nephrite minerals (Ling *et al.*, 2013; Zhang *et al.*, 2011; Chen *et al.*, 2004; Yu *et al.*, 2017; Siqin *et al.*, 2014). Nonetheless, because nephrite is not a monomineralic rock, its chemical compositions are likely to span greatly. Usually, the chemical data combining the inclusions can determine the mineralization type but hardly reveal the provenance due to the overlapping results (Qiu 2011; Yu *et al.*, 2016). Besides, for the same sample, different observation points or areas selected will also cause different final outcomes. This kind of non-uniformity exists locally in nephrite and makes analyzing method of trace elements loose the scope for displaying its abilities in the study of provenance (Ling *et al.*, 2015).

However, in the late years, some collectors and connoisseurs have found that nephrite from different provenances generally have different submicrostructure inside their bodies (Wang & Sun, 2013; Xiong 2009). This is a more significant characteristic than the texture on the scale, manly caused by coarse particles and aggregates of tremolite. The submicrostructure inside the nephrite can be perceived with naked eyes. As a kind of identification feature with important reference value, it is applied in daily market transactions, and as a valuable practical experience, it is only passed on by word of mouth. Under these circumstances, it has not been scientifically studied in the past, and even not been recorded reasonably and effectively with good images (Chen *et al.*, 2018).

We are committed to transforming this traditional experience into a more scientific presentation. After some tentative experiment and verification, the image of submicrostructure in the nephrite has be successfully recorded by multispectral technology, which makes a solid base for the exploration of nephrite provenance (Chen *et al.*, 2018). On this basis, this paper introduces that a series of optical and mathematical processing methods are further adopted to improve the quality of the image of submicrostructure, which can establish a reference standard and provide a more accurate and convenient judgment foundation for the market and collectors.

## 2. Experiments and methods

### *2.1. Nephrite samples*

The 12 pieces of raw nephrite samples come from the five most common sources in the Chinese market (Chen *et al.*, 2013; Prokhor 1991; Yui & Kwon 2002). They were provided by Prof. Ming Yu, in which 4 pieces were collected from original nephrite mines in Xinjiang, 2 from Qinghai and 2 from Liaoning Province, China. While other 2 pieces come from the East Sayan Mountains of Siberia, Russia, and 2 from Chuncheon in South Korea. The parts with good quality are cut from these raw nephrite materials and processed into small pieces of about 5cm×2cm×0.5cm for easy observation. The prepared samples are as shown in Fig. 1.

In order to keep similar conditions, the base color of selected nephrite is near to white as much as possible, ensuring that they belong to the same group in the traditional seven color categories. Besides, some nephrites from different sources have their own typical color characteristics, such as QH2 and XJ4 in Fig.1, which we have also taken into account in the standard of sample selection. The thickness for all samples is basically the same, so the effect of the sample size could be neglected. It should be emphasized that the distance of transmission light passing through nephrite should be kept as same as possible during measuring.

**Comment [M20]:** mono-mineralic

**Comment [M21]:** sub-microstructure

**Comment [M22]:** and

**Comment [M23]:** sub-microstructure

**Comment [M24]:** sub-microstructure

**Comment [M25]:** sub-microstructure

**Comment [M26]:** Methods

**Comment [M27]:** Samples

**Comment [M28]:** and

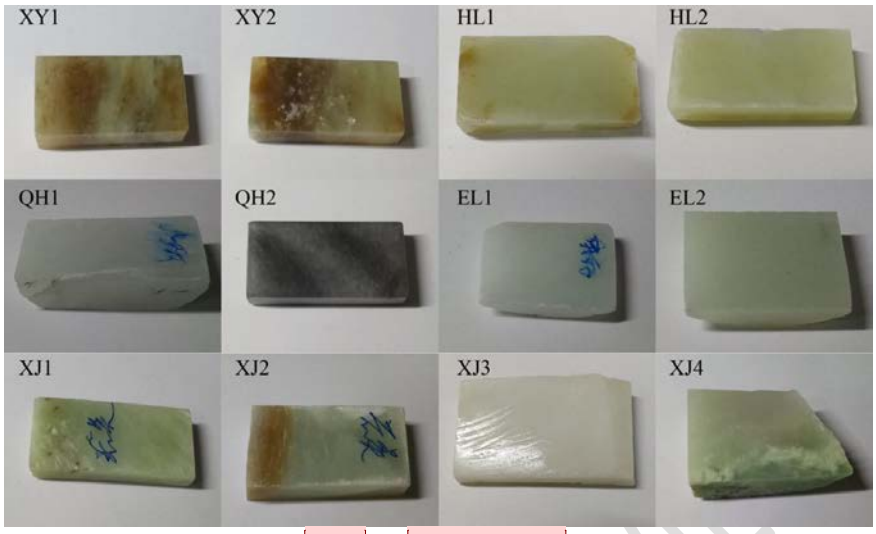


Fig. 1 The nephrite samples.

Note: XY for Xiuyan, Liaoning; QH for Qinghai; XJ for Xinjiang; HL for Chuncheon, South Korea and EL for Baikal, Russia.

*2.2. Multispectral imaging*

In recent years, the application of the multispectral imaging in the field of art conservation, art history and archaeology become more and more extensive. The multispectral imaging has the advantage of non-destructive and portable analysis and massive information of storage. A normal or standard imaging device could be applied to digitalize objects and re-create images as close to the original object or record both visible and invisible features (Imai *et al.*, 2002). For example, it has often been used in art galleries and libraries to reveal hidden texts and under-drawings. Moreover, convincing results had been achieved in material analysis and identification, preservation status assessment, digital image archive, and so on (Liang, 2012; Sitnik *et al.*, 2012).

This technology provides measurements in the UV, visible, near-infrared, and UV-fluorescence mode. UV spectra will rarely penetrate the surface, so they will be hardly influenced by the object material. On the other hand, IR spectra do penetrate deeper into the surface's material, and the degree of penetration will depend on the incident direction and the object material property (Hedjam & Cheriet 2013; Howell, 2018). In order to ensure that the information inside the object can be presented, white light is the better illumination choice (Liang, 2012). More specifically, the incident full optical band or wide band could be divided into several narrow optical beams, which irradiated the target objects and then each of beam will produce an image independently (Fischer & Kakoulli, 2006; Themelis *et al.*, 2008).

The multi-spectral imaging system model CRi Nuance made in USA was used in this study (Diebele *et al.*, 2012). The specific components are described in detail in our previous paper (Chen *et al.*, 2018). The images are acquired in the wavelength range of 450-740 nm with the scanning step of 10 nm, which covers the visible (VIS) and near-infrared (NIR). They are stored in a laptop connected to the camera. Subsequent processing of the images is performed by means of the CRi Nuance and Matlab programs.

To reduce diffuse reflectance and make light more uniform, the sample surface was smoothed on one side. The transmission light, produced by Light Emitting Diodes (LED), was adopted to

**Comment [M29]:** Fig. 1:

**Comment [M30]:** Nephrite Samples

**Comment [M31]:** and

**Comment [M32]:** and

illuminate the sample. Thus, the submicrostructure of the sample could be fully displayed in various bands. The sample was placed on the carrier platform at the proper height and angle to ensure that it would be within the field of view of the lens. The distance between the flat surface for all of samples and the lens is the same, the depth of field of focus will be consequently easier to be determined. The focal length of the lens was then adjusted until the image of the sample was clearly shown. The exposure parameters were preset and self-adjusted and the images will be recorded and saved by software.

As an example, a series of grayscale images are produced from different spectral band as shown in Fig. 2. Obviously, every image accepted distinct light energy. In particular, it can be found that the light source of LED has a greater impact on the image. When the light wavelength is about 600 nm, the brightness of the image will reach the highest. The structural textures of nephrite mainly depends on the gray difference of image to display, which may hard be visible to the naked eye in normal light. The aggregation of the structure and texture of nephrite on the scale of visible range is actually the so-called submicrostructure.

With the increase of wavelength, the image gradually changes from dark to light and then from light to dark. The quantitative results of their grey level histograms are presented in Fig. 3. The ordinate represents pixel value, and the abscissa represents grey level, where 0 means the darkest degree while 255 means the whitest in grey level. It can be seen that the grey level distribution has certain symmetry taking 600 nm receiving wavelength as centre. This pattern seems to be the general rule of nephrite samples. In most cases, the area with 0 grey level is the background which need to be discarded, whereas the brightest area is also invalid due to the high intensity of illumination. If there is an area with grey level higher than 230, the observation will be affected. Hence, histograms like band 600 nm do not meet the requirements. In addition, if the overall grey levels were set up more balanced, the original image will contain more details and gradations. Based on the above reasons, the moderate image of band 660 nm is selected as representatives in each series, and at the same time, the band of 510 nm could also be chosen due to symmetry.

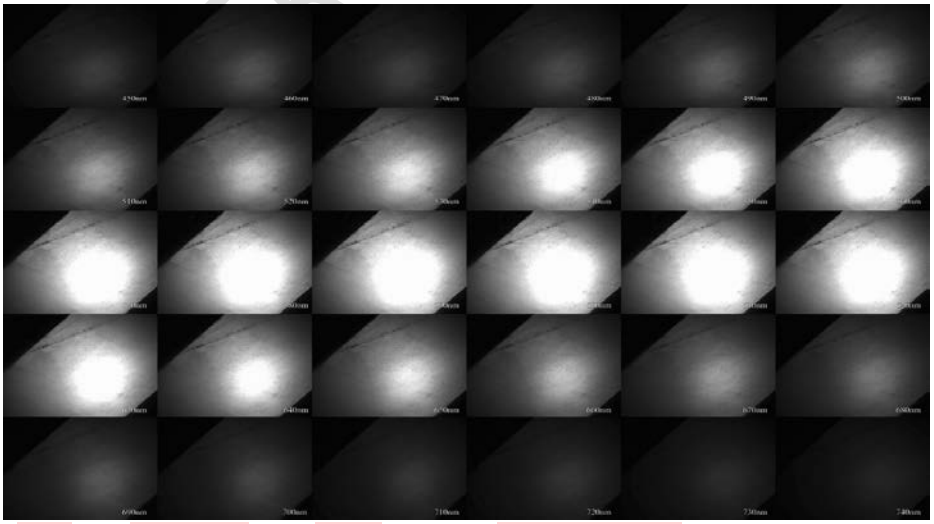

Fig. 2 Grey scale images of the sample (EL2) with wavelength ranging from 450 nm to 740 nm.



**Comment [M33]:** sub-microstructure

**Comment [M34]:** is in the

**Comment [M35]:** Delete

**Comment [M36]:** depend

**Comment [M37]:** sub-microstructure

**Comment [M38]:** levels

**Comment [M39]:** Fig, 2:

**Comment [M40]:** Scale Images

**Comment [M41]:** Sample

**Comment [M42]:** Wavelength Ranging

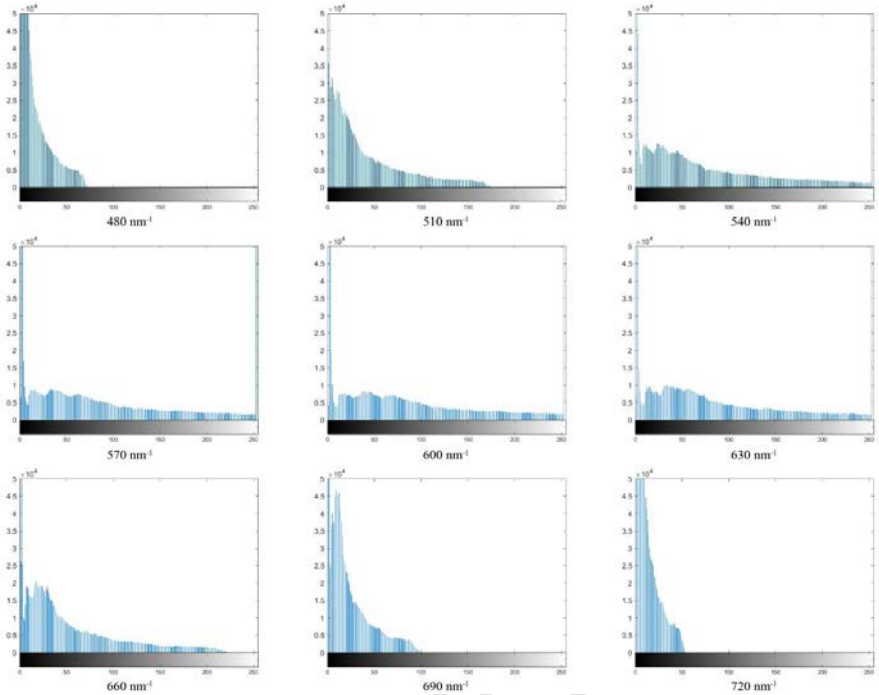


Fig. 3 Grey level histograms of a sample (EL2) with wavelength ranging from 480 nm to 720 nm (at 30 nm intervals).

Comment [M43]: Fig, 3:

Comment [M44]: Level Histograms

Comment [M45]: Sample

Comment [M46]: Wavelength Ranging

*2.3. Image enhancement*

Our basic idea is to regard the grey level image from multispectral data as a superposition of the illumination distribution and the target image. Hence, the most important step is to estimate the illumination distribution (Lin *et al.*, 2010). The smoothing linear filter method, a basic technique in image processing, was applied here. As a low-pass filter, the net effect is to blur or smooth an image such as bridging of small gaps in lines or curves. The value of each pixel in the image is replaced by the weighted average value which is the intensity levels in the neighborhood defined by the filter mask, this process will reduce abrupt transitions in an image (Gonzalez & Woods, 2008). The general implementation for filtering an $M \times N$ image giving different weights is given by the expression:

Comment [M47]: and

$$g(x,y) = \frac{\sum_{s=-at=-b}^{a}\sum^{b} w(s,t)\, f(x+s, y+t)}{\sum_{s=-at=-b}^{a}\sum^{b} w(s,t)} \quad \text{for} \quad x = 0,1,\ldots,M-1 \quad \text{and} \quad y = 0,1,\ldots,N-1.$$

where $f(x,y)$ and $g(x,y)$ are the grey values at the position $(x,y)$ of the original image and the processed image respectively while $\frac{w(s,t)}{\sum_{s=-at=-b}^{a}\sum^{b} w(s,t)}$ is the weight.

For simulating the distribution of illumination, the simplest way is to take the weight as the same, thus the filter becomes a mean filter (Sun, 2008). Generally speaking, the Gaussian filter is mainly used to depress noise which obeys normal distribution rather than blurring image. For avoiding discontinuity, the original grey levels on the boundary of pixels were reset to the same values. It must be noted that the definition of the same size for the filter mask should be crucial. In other words, the scale of the filter mask depends mainly on the size of details. It means that the distribution of image features in horizontal and vertical directions could be not very different, hence, the square filter mask is suitable choice.

Following, the filter masks of different sizes were compared (Fig. 4). To unify the standard, a region about 1×1cm$^2$ in the focused position of every image would be analyzed and processed by use of the software MATLAB (2018a). Different from other situations, here we want to emphasize the minor details in the image, which means that the proportion of 'effective information' we need is actually quite low. Therefore, many classical quantitative evaluation methods used to discriminate image enhancement or optimization are difficult to apply to this case. Although our operation is also subjective in some ways, it is consistent with actual experience. Rather than quantitative indicators, the guidcance from the collection circle will tend to contribute more to the image optimization. Here, we mainly take this subjective assessment to adjust the parameters.

It can be found from Fig. 4 that the clearness of sample edge is not greatly affected by mask size. Therefore, it is not necessary to intentionally select sample edges. In addition, if the filter mask is too small (10×10), the effective information will almost disappear. However, if the mask is too large (100×100), the processed image will be blurred. By virtue of experience, the optimal range of filter mask is between 30×30 and 50×50. However, for a particular image, the most suitable parameters are not exactly the same, but the filter mask around 40×40 is not much different. After comprehensive consideration, the 40×40 filter mask was selected in this research. Although this parameter is a subjective choice based on experience, it can greatly enhance the visual effect without deviating from the original image features.

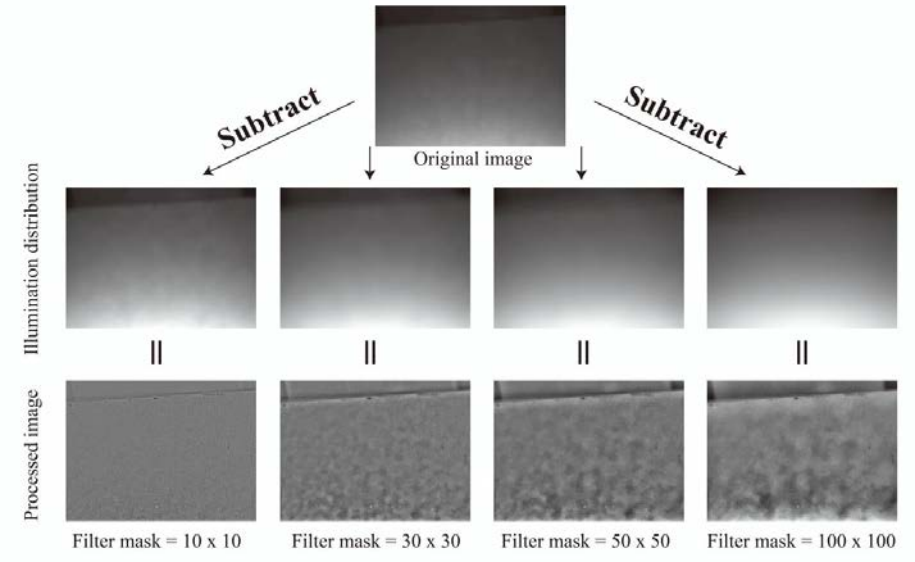


Fig. 4 Image processing sketch

Comment [M48]:

Comment [M49]: Fig. 4:

Comment [M50]: Processing Sketch

Note: first, subtracting illumination distribution from the original image is the processed image and then comparing the process effect by different filter mask (The sample HL1 nephrite is from Chuncheon).

## 3. Results and discussion

The submicrostructure image of nephrite appears mainly through different patches caused by different grey values, as shown in Fig. 4. In general, the structural features of nephrite from different sources have coherence. Referring to previous literatures (Wang & Sun, 2013; Li *et al.*, 2014), the significant image features of the nephrite from five sources are summarized in Table 1, where some descriptions are also combined with other sensory experience. Most importantly, the specific names to different submicrostructures are proposed, which can be used as an overview summary and description to some nephrite samples in the actual scene.

Table. 1 Comparison of the visual identification features of the nephrite from five sources.

| | Xinjiang | Qinghai | Xiuyan | Baikal | Chuncheon |
|---|---|---|---|---|---|
| Lustre | Strong grease gloss | Glass-wax gloss | Grease gloss | Grease gloss | Glass-wax gloss |
| Transparency | Slightly translucent | Semi-translucent and uneven | Slightly translucent | Slightly translucent | Slightly translucent |
| Submicrostructure | Flocculent textures | Granular scatter | Blurred pieces | Irregular patches | Round patches |
| Size | > 0.8 $cm^2$ | 0.05~0.1 $cm^2$ | > 0.8 $cm^2$ | > 0.6 $cm^2$ | 0.2~0.3 $cm^2$ |
| Distribution | Comparatively regular | Uniform | Slightly disorganized | Comparatively regular | Uniform |

From the micro-point of view, white nephrite from Xiuyan and South Korea with micro-fibrous interlocking texture, microfibre flaky blastic texture, microfibre granular crystalloblastic texture and porphyroblastic texture. Content of tremolite in nephrite from those areas is relatively slightly low, and fibers are coarse with large gap, which lead to rough texture and poor gloss in appearance and toughness decreasing (Wang & Sun, 2013; Li *et al.*, 2014).

The features embodied in processed grey scale images of nephrite from these two regions are in good agreement with visual perception. Under natural light, the naked eye can often observe a group of “patches” in Chuncheon nephrite. This corresponds with those bright white parts on grey level images (Fig. 4; HL1 and HL2 in Fig. 5). The “patches” are fairly uniform in size and approach to round shape with about 0.2~0.3 cm in diameter. Thus, its structure is called “round patches”, generally including its characteristics. Relatively speaking, the submicrostructure of Xiuyan nephrite seems more dim and hazy. The distribution of image features is less regular and the contrast of grey levels is not as fierce as that of Chuncheon nephrite. But Xiuyan nephrite has blending layers and gradual areas with size beyond 1 $cm^2$. The grey intensity remains almost constant in a certain preferential orientation while the depth of brightness alternates with its vertical direction, which is especially remarkable in XY2. For this reason, this kind of structure is termed as “blurred pieces”.

As for white nephrite and greyish nephrite from Xinjiang, as well as white nephrite with high quality from Russia, they usually have cryptocrystalline blastic texture with high content of tremolite from petrographic observation, where the fiber structure is small and closely intertwined. Therefore, these nephrite are fine, glossy in appearance and have higher degree of compaction, because their formation conditions may be more stable (Li *et al.*, 2014). They also definitely affect the submicrostructure to some extent.

Comment [M51]: Discussions
Comment [M52]: sub-microstructure
Comment [M53]: and
Comment [M54]: sub-microstructure
Comment [M55]: Table 1:
Comment [M56]: Visual
Comment [M57]: Identification
Comment [M58]: Nephrite
Comment [M59]: Five Sources
Comment [M60]: sub-microstructure
Comment [M61]: Removed/delete
Comment [M62]: sub-microstructure

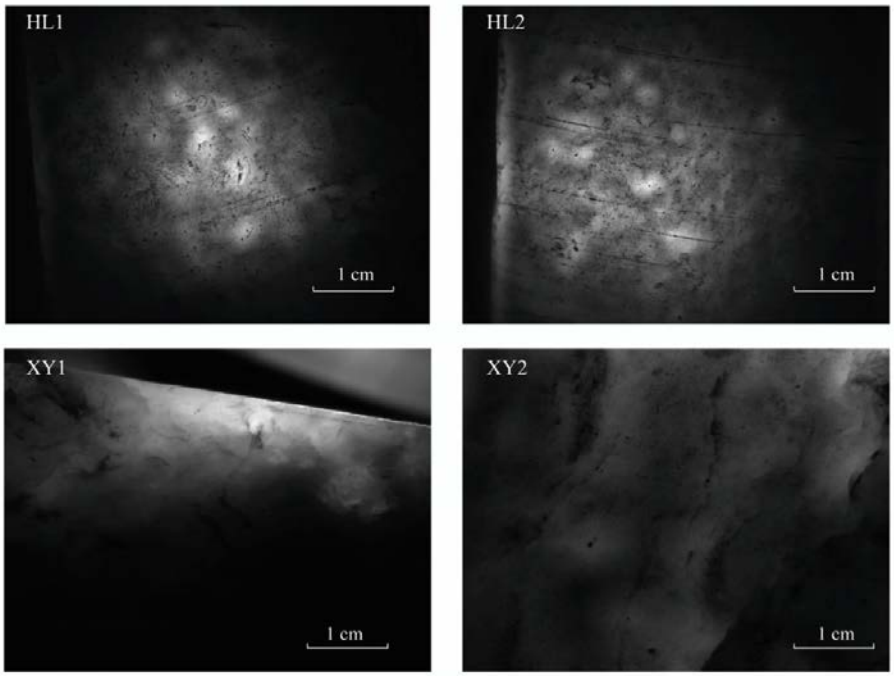


Fig. 5 The processed grey images of nephrite samples

Note: The samples HL1 and HL2 are from Chuncheon and XY1 and XY2 are from Xiuyan. The parallel lines appeared in HL1 and HL2 are traces left by cutting.

The characteristics of typical Qinghai white nephrite are very remarkable (QH1 and QH2 in Fig. 6). There are many bright spots with very small granularity. The distribution appear uniform and compact. A centimeter square can contain dozens of sugar-like spots. Therefore, it is referred to as “granular scatter”, which highlight the characteristics of large number and wide distribution. However, this feature obtained by the algorithm magnifies normal visual information which increases the discrimination degree of Qinghai nephrite. Slight variation also happened to Baikal nephrite compared with the actual situation. The image features include intertwining black and white areas with irregular shapes rather than smaller round patches of Chuncheon nephrite. Although some bright patches appear occasionally in Baikal nephrite, it only implies that its submicrostructure has comparatively poor homogeneity. This alternating grey levels and patches of different sizes seem to be compound characteristics of Xiuyan nephrite and Chuncheon nephrite. To differentiate, this structure was called as “irregular patches”.

**Comment [M63]:** Processed Grey Images

**Comment [M64]:** Nephrite Samples

**Comment [M65]:** appears

**Comment [M66]:** sub-microstructure

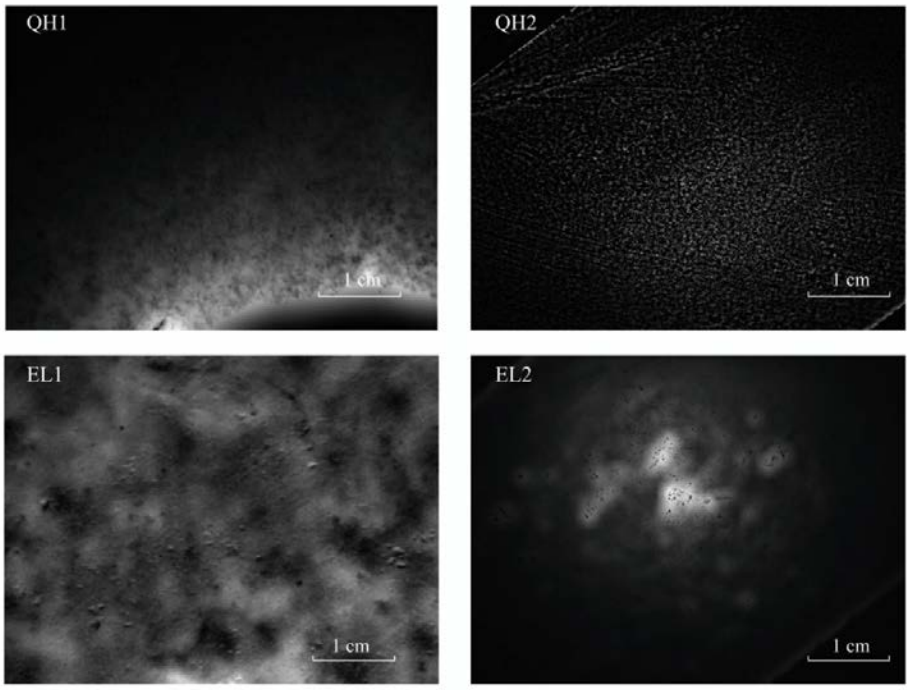


Fig. 6 The processed grey images of nephrite samples

Note: The samples QH1 and QH2 are from Qinghai and EL1 and EL2 are from Baikal.

Xinjiang nephrite usually has high quality and mild appearance. In Fig. 7, XJ1 and XJ3 show more dense and finer textures than those of Xiuyan nephrite. Whether bright or dark, the submicrostructure can be regarded as continuous areas. It may appear in different shapes, such as slices, strips, etc. It is worth mentioning that the filiform textures of XJ4 are not flaws or fractures in real vision, and it merely shows fine-grained regularity. To integrate the above features, this structure is called “flocculent texture”.

Most importantly, these processed images can be used for display and discussion with different experts in this research area. Thus, we can get feedback and incorporate the accumulated visual experience into scientific research. Besides, absorbing the traditional opinions will help us improve further optimization of images and modification of details in order to better carry out this idea for nephrite provenance identification.

Furthermore, it must be noted that previous scholars have noticed the microscopic texture when studying the toughness of nephrite, but this concept of structure did not have the same meaning with that in this paper, especailly due to the different observation methods and the magnifying power, where their results were based on TEM (Wang *et al.*, 1990; Dorling & Zussman, 1985). However, some findings could provide a certain explanation for the phenomena that we concerned. Several reasons contribute to the differences including the size of lath-like crystallites, azimuthal misorientations, irregular grain boundaries between laths within bundles and bundles of crystallites randomly oriented with irregular boundaries where they meet (Dorling & Zussman, 1985; Yu *et al.*, 2016). From a more geological genesis point of view, the submicroscopic characteristics in nephrite may have largely resulted from intra-and inter-grain

**Comment [M67]:** Processed grey Images

**Comment [M68]:** Nephrite Samples

**Comment [M69]:** sub-microstructure

**Comment [M70]:** especially

**Comment [M71]:** and

**Comment [M72]:** disorientation

**Comment [M73]:** and

slips, differential strain energy, oriented nucleation and growth in response to effective stresses (Dorling & Zussman, 1985).

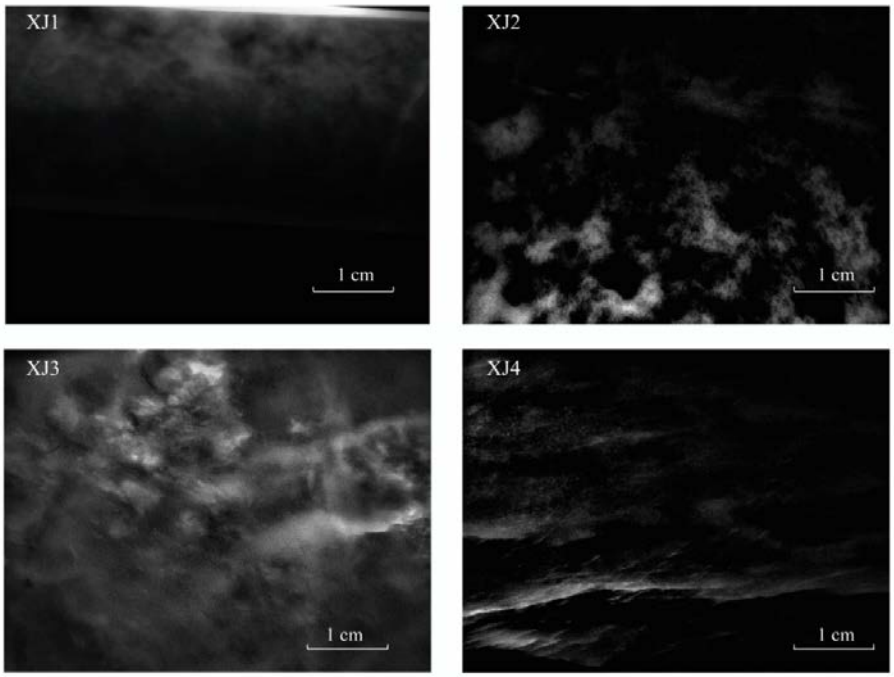


Fig. 7 The processed grey images of nephrite samples from Xinjiang

However, these statements are vague and there is no in-depth discussion and comparative analysis of nephrite from different sources in this perspective. In fact, there should be some intermediate explanations which may imply some relations to submicrostructure of nephrite. These mechanisms may have to be explored by researchers in the future.

**4. Conclusions**

This study shows that multispectral imaging technology and average filter algorithm can clearly reveal submicrostructure images of nephrite from different sources. These images correspond to the actual visual perception in some cases, while enhance and magnify the actual visual effect sometimes. On balance, the intuitive image features can finally match traditional experience, which will further support the feasibility of using image to discriminate the nephrite provenance.

Specifically, illumination could disturb the initial image. In this study, it was found that the images at wavelength 660 nm receive the least interference from the senses. Average filter with mask of 40×40 pixel size can successfully simulate uneven illumination distribution. Subtracting it from the original image obtained by multispectral imaging could generate the ideal effect image. Besides, these two parameters are strongly recommended. In light of above, nephrite samples from different sources show typical characteristics which are sufficient to determine the provenances.

Furthermore, the submicrostructures of nephrite are named respectively, and the traditional visual characteristics including the shape, size and distribution have also been summarized. The differences of submicrostructure are more obvious and direct than those in appearance. But the specific mechanism of different submicrostructures still needs to be clarified. This study lays a

**Comment [M74]:** and

**Comment [M75]:** Processed Grey Images

**Comment [M76]:** Nephrite Samples

**Comment [M77]:** sub-microstructure

**Comment [M78]:** sub-microstructure

**Comment [M79]:** sub-microstructures

**Comment [M80]:** sub-microstructure

**Comment [M81]:** sub-microstructures

solid foundation for identifying the provenances of nephrite by image, and facilitates the introduction of more quantitative means in the future.

## References


Bukanov, V.V., (2006): Russian Gemstones Encyclopedia, Saint-Petersburg Press, p.472.

Chen, D., Pan, M., Huang. W, Luo, W.G., Wang, C.S., (2018): The provenance of nephrite in china based on multi-spectral imaging technology and gray-level co-occurrence matrix. *Analytical Methods*, **10**, 4053-4062.

Chen, Q., Bao, D., Yin, Z., (2013): Study on xrd and infrared spectroscopy of nephrites from xinjiang and xiuyan, liaoning. *Spectroscopy & Spectral Analysis*, **33**(11), 3142-3146.

Chen, T.H., Calligaro, T., Pagès-Camagna, S., Menu, M., (2004): Investigation of Chinese archaic jade by PIXE and μRaman spectrometry. *Applied Physics A*, **79**, 177-180.

Diebele, I., Bekina, A., Derjabo, A., Kapostinsh, J., Kuzmina, I., Spigulis, J., (2012): Analysis of skin basalioma and melanoma by multispectral imaging. *Proceedings of SPIE -The International Society for Optical Engineering*, **8427(2)**, 63.

Dorling, M., Zussman, J., (1985): An investigation of nephrite jade by electron microscopy. *Mineralogical Magazine*, 49: 31-36.

Fischer, C., Kakoulli, I., (2006): Multispectral and hyperspectral imaging technologies in conservation: current research and potential applications. *Studies in Conservation*, **51**, 3-16.

Gonzalez, R.C., Woods, R.E., (2008): Digital image processing, Prentice Hall, Upper Saddle River, N.J.

Harlow, G.E., Sorensen, S.S., (2005): Jade (nephrite and jadeitite) and serpentinite: metasomatic connections. *International Geology Review*, **47**, 113-146.

Hawthorne, F.C., Oberti, R., (2006): On the classification of amphiboles. *The Canadian Mineralogist*, **44**: 1-21.

Hedjam, R., Cheriet, M., (2013): Historical document image restoration using multispectral imaging system. *Pattern Recognition*, **46**, 2297-2312.

Howell, D., (2018): The potential of hyperspectral imaging for researching colour on artefacts. Digital Imaging of Artefacts: Developments in Methods, 37-48, Archaeopress Access Archaeology.

Imai, F.H., Rosen, M.R., Berns, R.S., (2002): Comparative Study of Metrics for Spectral Match Quality. Conference on Colour in Graphics, 2002, **5**, 492-496.

Lu, L., Bian, Z.H., Wang, F., Wei, J.Q., Ran, X.H., (2014): Comparative study on mineral components, microstructures and appearance characteristics of nephrite from different origins. *Journal of Gems & Gemmology*, **16**(2).

Liang, H.D., (2012): Advances in multispectral and hyperspectral imaging for archaeology and art conservation. *Applied Physics A*, **106**, 309-323.

Lin, L., He, W.P., Lei, L., Zhang, W., Wang, H.X., (2010): Survey on enhancement methods for non-uniform illumination image. *Application Research of Computers*, **27**(5), 1625-1628.

Ling, X.X., Schmädicke, E., Li, Q.L., Gose, J., Wu, R.H., Wang, S.Q., Liu, Y., Tang, G.Q., Li, X.H., (2015): Age determination of nephrite by in-situ SIMS U–Pb dating syngenetic titanite: A case study of the nephrit deposit from Luanchuan, Henan, China. *Lithos*, Volumes 220-223, 289-299.

Ling, X.X., Schmädicke, E., Wu, R.H., Wang, S.Q., Gose, J., (2013): Composition and distinction of white nephrite from Asian deposits. *Neues Jahrbuch für Mineralogie*, **190**, 49-65.

Liu, Y., Deng, J., Shi, G.H., Yui, T.F., Zhang, G.B., Abuduwayiti, M., Yang, L.Q., Sun, X., (2011): Geochemistry and petrology of nephrite from Alamas, Xinjiang, NW China. *Journal of Asian Earth Sciences*, **42**, 440-451.

Prokhor, S.A., (1991): The genesis of nephrite and emplacement of the nephrite-bearing ultramafic complexes of east sayan. *International Geology Review*, (**3**), 290-300.




**Comment [M82]:** P

**Comment [M83]:** N

**Comment [M84]:** C

**Comment [M85]:** B

**Comment [M86]:** M

**Comment [M87]:** I

**Comment [M88]:** T

**Comment [M89]:** G

**Comment [M90]:** C

**Comment [M91]:** M

**Comment [M92]:** NOTE ALL FIRST MAIN WORD SHOULD BE IN CAPITAL LETTER

**Comment [M93]:** NOTE ALL FIRST MAIN WORD SHOULD BE IN CAPITAL LETTER

**Comment [M94]:** Removed the bold?

**Comment [M95]:** NOTE ALL FIRST MAIN WORD SHOULD BE IN CAPITAL LETTER

**Comment [M96]:** NOTE ALL FIRST MAIN WORD SHOULD BE IN CAPITAL LETTER

**Comment [M97]:** NOTE ALL FIRST MAIN WORD SHOULD BE IN CAPITAL LETTER

**Comment [M98]:** NOTE ALL FIRST MAIN

**Comment [M99]:** NOTE ALL FIRST MAIN

**Comment [M100]:** NOTE ALL FIRST MAIN

**Comment [M101]:** NOTE ALL FIRST MAIN

**Comment [M102]:** NOTE ALL FIRST MAIN

**Comment [M103]:** NOTE ALL FIRST MAIN

**Comment [M104]:** NOTE ALL FIRST MAIN

**Comment [M105]:** NOTE ALL FIRST MAIN

**Comment [M106]:** NOTE ALL FIRST MAIN

**Comment [M107]:** NOTE ALL FIRST MAIN

**Comment [M108]:** NOTE ALL FIRST MAIN

Qiu, Z.L., (2011): Enclaves in jades and jade material concept, category and fingerprints for indicating jade's origin. China Jewelry Academic Exchange.

Siqin, B., Qian, R., Zhuo, S., Gao, J., Jin, J., Wen, Z.Y., (2014): Studies of rare earth elements to distinguish nephrite samples from different deposits using direct current glow discharge mass spectrometry. Journal of *Analytical Atomic Spectrometry*, **29**, 2064-2071.

Sitnik, R., Jakub, K., Grzegorz, M., (2012): Archiving shape and appearance of cultural heritage objects using structured light projection and multispectral imaging. *Optical Engineering*, **51**, 1115.

Sun, Z.G., (2008): Reduce Non-uniform Illumination Achieved by Matlab, *Microcomputer information*, **24**(12).

Themelis, G., Yoo, J.S., Ntziachristos, V., (2008): Multispectral imaging using multiple-bandpass filters. *Optics Letters*, **33**, 1023-1025.

Wang, C.Y., Zhang, H.F., Ren, G.H., (1990): Sub-microscopic textures and retrogressive metamorphic origin of Longxi nephrite. Chin. *J. of Geochem*, **9**: 182-187.

Wang, S.Q., Sun, L.H., (2013): Visual Identification of Tremolite Features of Five Origins in Today's Nephrite Jade Market. China Symposium on jewellery academic exchange, Beijing, China (in Chinese with English abstract).

Wen, G., Jing, Z.C., (1992): Chinese neolithic jade: a preliminary geoarchaeological study. *Geoarchaeology*, **7**, 251-275.

Xiong, Y., (2009): Differences in structure and appearance of white nephrite from Xinjiang, Qinghai, Russia and Korea. Master's thesis, China University of Geosciences (Wuhan).

Yang, H., Liu, G.H., (2017): Apreliminary discussion on Xinglongwa jades, in The Origin of Jades in East Asia (Jades of the Xinglongwa Culture). Chinese University of Hong Kong Press, Hong Kong, 210-216.

Yu, H., Wang, R., Guo, J., Li, J., Yang, X., (2016): Color–inducing elements and mechanisms in nephrites from Golmud, Qinghai, NW China: Insights from spectroscopic and compositional analyses. *Journal of Mineralogical & Petrological Sciences*, **111**, 313-325.

Yu, H.Y., Wang, R.C., Guo, J.C., Li J.G., Yang, X.W., (2016): Study of the minerogenetic mechanism and origin of Qinghai nephrite from Golmud, Qinghai, Northwest China. *Sci. China Earth Sci*, **59**: 1597-1609.

Yu, J., Hou, Z., Sahar, S., Dong, J., Han, W., Lu, T.J., Wang, Z., (2017): Provenance classification of nephrite jades using multivariate LIBS; a comparative study. *Analytical Methods*, **10**(3).

Yui, T. F., Kwon, S.T., (2002): Origin of a dolomite-related jade deposit at chuncheon, korea. *Economic Geology*, **97**(3), 593-601.

Zhang, Z.W., Gan, F.X., Cheng, H.S., (2011): PIXE analysis of nephrite minerals from different deposits. *Nuclear Instruments and Methods in Physics Research B*, **269**, 460-465.



**Comment [M109]:** NOTE ALL FIRST MAIN WORD SHOULD BE IN CAPITAL LETTER

**Comment [M110]:** NOTE ALL FIRST MAIN WORD SHOULD BE IN CAPITAL LETTER

**Comment [M111]:** NOTE ALL FIRST MAIN WORD SHOULD BE IN CAPITAL LETTER

**Comment [M112]:** NOTE ALL FIRST MAIN WORD SHOULD BE IN CAPITAL LETTER

**Comment [M113]:** NOTE ALL FIRST MAIN WORD SHOULD BE IN CAPITAL LETTER

**Comment [M114]:** NOTE ALL FIRST MAIN WORD SHOULD BE IN CAPITAL LETTER

**Comment [M115]:** NOTE ALL FIRST MAIN WORD SHOULD BE IN CAPITAL LETTER

**Comment [M116]:** NOTE ALL FIRST MAIN WORD SHOULD BE IN CAPITAL LETTER

**Comment [M117]:** NOTE ALL FIRST MAIN WORD SHOULD BE IN CAPITAL LETTER

**Comment [M118]:** NOTE ALL FIRST MAIN WORD SHOULD BE IN CAPITAL LETTER

**Comment [M119]:** NOTE ALL FIRST MAIN WORD SHOULD BE IN CAPITAL LETTER

**Comment [M120]:** Korea

**Comment [M121]:** NOTE ALL FIRST MAIN WORD SHOULD BE IN CAPITAL LETTER

**Comment [M122]:** NOTE ALL FIRST MAIN WORD SHOULD BE IN CAPITAL LETTER